IIAI Open Conference Publication Series
IIAI Letters on Informatics and Interdisciplinary Research
Vol.006, LIIR428
DOI: https://doi.org/10.52731/liir.v006.428

Proposal of an SEIR Model Considering Inter-population Transfers and Vaccine Availability in Large Populations

Hiroyoshi Matsumoto [*], Yusuke Yamauchi [*],
Shimpei Matsumoto [*]

Abstract

This study proposes an infectious disease model incorporating person-trip data and adopts an extended SEIR framework based on the classical SIR model. The analysis specifically targets the spread of the Omicron variant of COVID-19, which proliferated across Japan in the early months of 2022. Following the construction of a SEIR-based epidemiological model, a single infectious region is segmented into four distinct groups to simulate diverse transmission dynamics through person-trip movements. Using empirical records of infection cases and commuter flows in Saitama, Tokyo, Kanagawa, and Chiba prefectures from January to April 2022, the model estimates key parameter values, including infection rate, recovery rate, and mobility rate. Additionally, vaccine efficacy parameters released by the Ministry of Health, Labour and Welfare are incorporated into the simulation. Based on the estimated parameters, the study investigates the potential for mitigating the spread of infection. The model's validity is then assessed by comparing the simulated data of new infections with actual epidemiological data from the aforementioned four prefectures used in the parameter estimation. Furthermore, the study explores various scenarios by altering the parameters related to human mobility and vaccine efficacy to evaluate which preventive measure—mobility restriction or immunity acquisition through vaccination—more effectively curtails the spread of infection.

Keywords: SEIR model, Epidemic model, Person trip, Covid_19, Vaccine,

1 Introduction

The COVID-19 pandemic has wreaked havoc globally, including in Japan, with a total of 33,803,572 infections and 74,694 deaths recorded as of December 31, 2023. As of January 2025, although the momentum of infections has diminished compared to the early stages of the outbreak, measures still need to be taken.

The SIR (Susceptible-Infectious-Recovered) model, formulated by Kermack and McKendrick in 1927, represents the short-term epidemic process of infectious diseases through classical model equations (1). The SIR model assumes the absence of immunity to the novel infectious disease, no population movement between external cities, population density with contact with an unspecified large number of people, and a rapid and short-term outbreak like the plague. The name is derived from the initials of the susceptible individuals (S), infected individuals (I), and recovered or removed individuals (R). On the other hand, the SEIR model extends the SIR model by considering exposed individuals (E) due to the infectious disease (2). During the Ebola virus outbreak in West Africa from 2014 to 2015, an extension of the SIR model was applied to epidemic analysis to suppress infection spread (3).

[*] Hiroshima Institute of Technology, Hiroshima, Japan

The differential equations for each model are as follows:

$$\frac{dS}{dt}(t) = -\frac{\alpha S(t)I(t)}{N}$$

$$\frac{dI}{dt}(t) = \frac{\alpha S(t)I(t)}{N} - \beta I(t)$$

$$\frac{dR}{dt}(t) = \beta I(t)$$

$$\frac{dS}{dt}(t) = -\frac{\alpha S(t)I(t)}{N}$$

$$\frac{dE}{dt}(t) = \frac{\alpha S(t)I(t)}{N} - \varepsilon E(t)$$

$$\frac{dI}{dt}(t) = \varepsilon E(t) - \beta I(t)$$

$$\frac{dR}{dt}(t) = \beta I(t)$$

Figure1: Differential equations for SIR and SEIR models

The investigation of human mobility within specific regions—such as intercity movements—is referred to as a "person trip survey." Previous research (3) employed this concept to conduct numerical analyses focused on influenza. That study examined various intercity movements from the perspective of person trip surveys, derived the next-generation matrix, and calculated the basic reproduction number as well as city-specific reproduction numbers.

However, considering that the aforementioned research primarily addressed influenza, certain contextual discrepancies may arise when compared to the current focus on COVID-19. The SIR (Susceptible-Infectious-Recovered) model posits that susceptible individuals (S) contract the infection directly from infectious individuals (I). In reality, however, infectious individuals (I) are typically isolated immediately upon testing positive, making it improbable for them to directly influence susceptible individuals (S). Consequently, this study assumes that the influence on susceptible individuals (S) is primarily exerted by exposed individuals (E), who are in the latent phase of infection.

Moreover, to investigate the impact of human mobility on the spread of infection, the study restricts mobility to occur solely among four defined population groups.

Many studies utilizing the SIR model operate under the assumption of a constant contact rate, denoted by α. However, in human societies characterized by dynamic social behavior, the assumption of a temporally constant contact rate diverges from empirical realities. Therefore, this study constructs an SEIR model predicated on the assumption that population movement occurs only during daytime hours.

Key parameters—including vaccine effectiveness, infection rate, and initial conditions—are derived from actual data provided by the Ministry of Health, Labour and Welfare, as well as infection and commuting data from the Saitama, Tokyo, Kanagawa, and Chiba prefectures. These are compared and analyzed in relation to observed infection trends. Furthermore, acknowledging that vaccine administration inherently necessitates human movement, the study explores, based on empirical data, the threshold level of vaccine efficacy at which the benefits of administration outweigh the risks associated with mobility. Based on these analyses, the study deliberates on public health measures that may be considered effective in mitigating the spread of infectious diseases.

2 Concept

This section provides a comprehensive exposition of the SEIR model employed in the present study. The model incorporates person trips, diurnal variations in human mobility affecting contact rates, and the efficacy of vaccination. The equations derived herein constitute the foundational framework for the numerical computations and simulations conducted to analyze the spread of the COVID-19 Omicron variant within Japan.

2.1 Prerequisite

The period referenced in the construction of this model corresponds to the phase during which epidemic containment measures were actively enforced, under the presumption that only essential outings—such as commuting to work or school—were undertaken. Consequently, individuals traveling from foreign countries or other prefectures are excluded from consideration. Parameters associated with demographic dynamics, including reinfection, birth, and mortality, are not incorporated due to the structural limitations of the SEIR model. Additionally, the potential immunological enhancement resulting from prior infection is not accounted for. Furthermore, asymptomatic carriers, whose presence is inherently difficult to detect and whose influence on susceptible individuals remains ambiguous, are excluded from the scope of this model.

All initial values employed within the model are derived exclusively from datasets published by national and local governmental authorities.

The authors undertake an analytical exploration of the effects of human mobility and vaccination on the propagation of infectious disease using this model.

2.2 Epidemic Model

This section formulates the extension of the SIR model using person trips. The Kermack-Mckendrick SIR model serves as the foundation of this epidemic model. The SIR model categorizes the population of an epidemic region into three compartments: "susceptible," "infectious," and "recovered." The SIR model employs a system of coupled differential equations to represent transitions between these compartments. S, I, and R represent susceptible, infectious, and recovered individuals, respectively, where S denotes the number of susceptible individuals, I denotes the number of infectious individuals, and R denotes the number of recovered individuals. The difference between S and I is proportional to the number of susceptible individuals in contact with infectious individuals. Additionally, the difference between I and R is proportional to the number of infectious individuals. Therefore, the differences among S, I, and R are expressed by the following equations.

To resolve these issues using the SEIR model, the epidemic area is partitioned into four groups, defining the susceptible, infected, and recovered individuals of Group 1 as S1, E1, I1, R1.

Furthermore, this framework accommodates different infectious diseases per person trip. α_1 denotes the infection rate of Group 1, β_1 signifies the recovery rate of Group 1, N_1 represents the total population in that group (S1 + E1 + I1 + R1), and T12 denotes the migration rate from Group 1 to Group 2.

Let λ represent the number of new infections during the daytime in Group 1. The number of susceptible individuals in Group 1 during the daytime is denoted as $S_1^d(t)\frac{T_{1,1}}{N_1^d}$. The count of infected individuals in Group 1 during the daytime is given by $S_1^d(t)\frac{T_{1,1}}{N_1^d}$, obtained from

the migration rate from Group 1 to Group 1, denoted as T1.1, and the daytime population N_1 of Group 1. The number of latent individuals moving to Group 1 during the daytime is provided for Groups 1 through 4, denoted as $T_{1\sim4,1}E_{1\sim4}$ and the total number of latent individuals moving from all groups to Group 1 is given as $\left(T_{1,1}E_1(t) + T_{2,1}E_2(t) + T_{3,1}E_3(t) + T_{4,1}E_4(t)\right)$. Let ω denote the vaccine efficacy and α_1 represent the infection rate of Group 1. Under these conditions, the number of susceptible individuals who become newly infected is expressed by the following equation:
$S_1^d(t)\frac{T_{1,1}}{N_1^d}\alpha_1\omega\left(T_{1,1}E_1(t) + T_{2,1}E_2(t) + T_{3,1}E_3(t) + T_{4,1}E_4(t)\right)$.

By substituting the above expressions from Groups 1 through 4, the following equations are derived.

$$\lambda_1^d = S_1^d(t)\frac{T_{1.1}}{N_1^d}\alpha_1\omega\left(T_{1,1}E_1(t) + T_{2,1}E_2(t) + T_{3,1}E_3(t) + T_{4,1}E_4(t)\right)$$

$$+S_1^d(t)\frac{T_{1,2}}{N_2^d}\alpha_2\omega\left(T_{1,2}E_1(t) + T_{2,2}E_2(t) + T_{3,2}E_3(t) + T_{4,2}E_4(t)\right)$$

$$+S_1^d(t)\frac{T_{1,3}}{N_3^d}\alpha_3\omega\left(T_{1,3}E_1(t) + T_{2,3}E_2(t) + T_{3,3}E_3(t) + T_{4,3}E_4(t)\right)$$

$$+S_1^d(t)\frac{T_{1,4}}{N_4^d}\alpha_4\omega\left(T_{1,4}E_1(t) + T_{2,4}E_2(t) + T_{3,4}E_3(t) + T_{4,4}E_4(t)\right) \quad (1)$$

Let λ_1^n denote the number of new infections occurring during the nighttime. Under the assumption that no inter-group movement takes place at night, the susceptible individuals present during this period are represented by S_1^n. This quantity is determined by the vaccine efficacy ω, the infection rate α_1 of Group 1, the number of exposed individuals E_1, the total nighttime population N_1 of Group 1, and the secondary infection rate within household contacts, denoted as h(4).

The secondary infection rate within households is referenced from data provided by the National Institute of Infectious Diseases. The institute calculates the secondary infection rate within households (PCR positivity rate among close contacts) based on the basic attributes and contact history of infected individuals and close contacts within households (including non-family members).

The following equation calculates the number of new infections during the nighttime in Group 1.

$$\lambda_1^n = \alpha_1 h\omega\frac{S_1^n(t)}{N_1^n}E_1(t) \quad (2)$$

To determine the number of new infections λ_1 in Group 1, the following equation is derived by calculating the average of the sum of the daytime new infections λ_1^d in Group 1 and the nighttime new infections λ_1^n in Group 1.

$$\lambda_1(t) = \frac{1}{2}(\lambda_1^d + \lambda_1^n) \quad (3)$$

Let S_1 represent the susceptible individuals in Group 1, and as susceptible individuals in Group 1 transition to newly infected individuals, the number of susceptible individuals decreases, denoted as $-\lambda_1(t)$.

$$\frac{dS_1}{dt}(t) = -\lambda_1(t) \quad (4)$$

The latent period of the COVID-19 Omicron variant, the subject of this study, has been disclosed to be approximately 3 days, according to the data published by the National Institute of Infectious Diseases (5). Therefore, it is assumed that individuals who are susceptible in this study will develop symptoms precisely 3 days after being infected by latent individuals. Consequently, the number of latent individuals, denoted as E_1 (t) in Group 1, is the sum of individuals in latent period 1 ($E_{1.1}$ (t)), latent period 2 ($E_{1.2}$ (t)), and latent period 3 ($E_{1.3}$ (t)). The following is a list of

$$E_1(t) = E_{1.1}(t) + E_{1.2}(t) + E_{1.3}(t) \quad (5)$$

Let $E_{1.1}$ denote individuals in Group 1 on the first day of the latent period. There is no data available on latent individuals in the data disclosed by the government or prefectures. This is because latent individuals have not yet developed symptoms, making it difficult to observe them as latent individuals. In my SEIR model, as mentioned earlier, susceptible individuals are assumed to become infectious three days after infection. Therefore, in the data disclosed by the government or prefectures, it is assumed that the number of new infections corresponds to the first day of the latent period two days prior to symptom onset.

Furthermore, since we are interested only in individuals on the first day of the latent period ($E_{1.1}$), the formula for$E_{1.1}$is derived by subtracting the number of individuals on the first day of the latent period from the number of new infections disclosed daily, obtained by subtracting the number of individuals on the first day of the latent period from the number of new infections disclosed daily.

$$\frac{dE_{1.1}}{dt}(t) = \lambda_1(t) - E_{1.1}(t) \quad (6)$$

(7) coincides with the aforementioned content, yet designates individuals in Group 1 on the second day of the latent period as E1.2. Individuals on the first day of the latent period transition to those on the second day of the latent period the following day. Hence, subtracting the number of old second-day latent individuals from the number of new second-day latent individuals results in the count of second-day latent individuals on day t.

$$\frac{dE_{1.2}}{dt}(t) = E_{1.1}(t) - E_{1.2}(t) \quad (7)$$

(8) overlaps with the aforementioned information, designating individuals in Group 1 on the third day of the latent period as E1.3. Individuals on the second day of the latent period transition to those on the third day of the latent period the following day. Therefore, subtracting the number of old third-day latent individuals from the number of new third-day latent individuals results in the count of third-day latent individuals on day t.

$$\frac{dE_{1.3}}{dt}(t) = E_{1.2}(t) - E_{1.3}(t) \quad (8)$$

Let I_1 represent the infected individuals in Group 1. The infected individuals in Group 1 are those who were in the third day of the latent period the previous day. Additionally, among the infected individuals, there are those who recover from the infection and no longer remain infected. Those who have recovered from the infection are designated as recoveries (σ_1 or R_1). Infected individuals continue to accumulate as such until they recover from the infection.

$$\frac{dI_1}{dt}(t) = E_{1.3}(t-1) - \sigma_1 = I_1(t) - \sigma_1 \quad (9)$$

R_1 represents the daily number of recoveries in Group 1, where β denotes the recovery

rate, and $I_1(t)$ represents the number of infected individuals. Multiplying these two yields the daily number of recoveries for Group 1. This is illustrated below.

$$\frac{dR_1}{dt}(t) = \sigma_1(t) \quad (10)$$

β represents the recovery rate, and $I_1(t)$ denotes the infected individuals. These two variables allow us to calculate the daily number of recoveries for Group 1. This is illustrated below.

$$\sigma_1(t) = \beta I_1(t) \quad (11)$$

The above elucidates equations (1) through (11) for Group 1. The equations for Groups 2, 3, and 4 involve merely substituting parameters such as initial values and coefficients with the values from Group 1, hence, explanation is omitted. The following is a list of

$$\frac{dS_1}{dt}(t) = -\lambda_1(t) \quad (4)$$

$$\frac{dE_{1.1}}{dt}(t) = \lambda_1(t) - E_{1.1}(t) \quad (6)$$

$$\frac{dE_{1.2}}{dt}(t) = E_{1.1}(t) - E_{1.2}(t) \quad (7)$$

$$\frac{dE_{1.3}}{dt}(t) = E_{1.2}(t) - E_{1.3}(t) \quad (8)$$

$$\frac{dI_1}{dt}(t) = E_{1.3}(t-1) - \sigma_1 = I_1(t) - \sigma_1 \quad (9)$$

$$\frac{dR_1}{dt}(t) = \sigma_1(t) \quad (10)$$

※ supplementation

$$\lambda_1^g = S_1^g(t)\frac{T_{1,1}}{N_1^g}\alpha_1\omega\left(T_{1,1}E_1(t) + T_{2,1}E_2(t) + T_{3,1}E_3(t) + T_{4,1}E_4(t)\right)$$
$$+S_1^g(t)\frac{T_{1,2}}{N_2^g}\alpha_2\omega\left(T_{1,2}E_1(t) + T_{2,2}E_2(t) + T_{3,2}E_3(t) + T_{4,2}E_4(t)\right)$$
$$+S_1^g(t)\frac{T_{1,3}}{N_3^g}\alpha_3\omega\left(T_{1,3}E_1(t) + T_{2,3}E_2(t) + T_{3,3}E_3(t) + T_{4,3}E_4(t)\right)$$
$$+S_1^g(t)\frac{T_{1,4}}{N_4^g}\alpha_4\omega\left(T_{1,4}E_1(t) + T_{2,4}E_2(t) + T_{3,4}E_3(t) + T_{4,4}E_4(t)\right) \quad (1)$$

$$\lambda_1^n = \alpha_1 h\omega\frac{S_1^n(t)}{N_1^n}E_1(t) \quad (2)$$

$$\lambda_1(t) = \frac{1}{2}(\lambda_1^g + \lambda_1^n) \quad (3)$$

$$E_1(t) = E_{1.1}(t) + E_{1.2}(t) + E_{1.3}(t) \quad (5)$$

$$\sigma_1(t) = \beta I_1(t) \quad (11)$$

Figure 2: SEIR model for Group 1

$$\frac{dS_2}{dt}(t) = -\lambda_2(t) \quad (12)$$

$$\frac{dE_{2.1}}{dt}(t) = \lambda_2(t) - E_{2.1}(t) \quad (13)$$

$$\frac{dE_{2.2}}{dt}(t) = E_{2.1}(t) - E_{2.2}(t) \quad (14)$$

$$\frac{dE_{2.3}}{dt}(t) = E_{2.2}(t) - E_{2.3}(t) \quad (15)$$

$$\frac{dI_2}{dt}(t) = E_{2.3}(t-1) - \sigma_2 = I_2(t) - \sigma_2 \quad (16)$$

$$\frac{dR_2}{dt}(t) = \sigma_2(t) \quad (17)$$

※ supplementation

$$\lambda_2^g = \lambda_2^g = S_2^g(t)\frac{T_{2,1}}{N_2^g}\alpha_1\omega\left(T_{1,1}E_1(t) + T_{2,1}E_2(t) + T_{3,1}E_3(t) + T_{4,1}E_4(t)\right)$$
$$+S_2^g(t)\frac{T_{2,2}}{N_2^g}\alpha_2\omega\left(T_{1,2}E_1(t) + T_{2,2}E_2(t) + T_{3,2}E_3(t) + T_{4,2}E_4(t)\right)$$
$$+S_2^g(t)\frac{T_{2,3}}{N_3^g}\alpha_3\omega\left(T_{1,3}E_1(t) + T_{2,3}E_2(t) + T_{3,3}E_3(t) + T_{4,3}E_4(t)\right)$$
$$+S_2^g(t)\frac{T_{2,4}}{N_4^g}\alpha_4\omega\left(T_{1,4}E_1(t) + T_{2,4}E_2(t) + T_{3,4}E_3(t) + T_{4,4}E_4(t)\right) \quad (18)$$

$$\lambda_2^n = \alpha_2 h\omega\frac{S_2^n(t)}{N_2^n}E_2(t) \quad (19)$$

$$\lambda_2(t) = \frac{1}{2}(\lambda_2^g + \lambda_2^n) \quad (20)$$

$$E_2(t) = E_{2.1}(t) + E_{2.2}(t) + E_{2.3}(t) \quad (21)$$

$$\sigma_2(t) = \beta I_2(t) \quad (22)$$

Figure 3: SEIR model for Group2

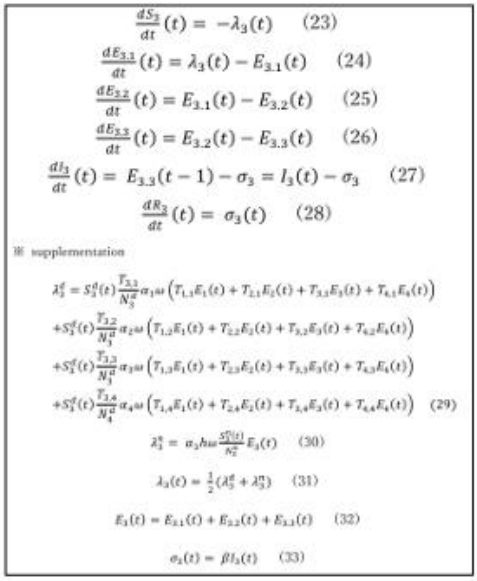

$$\frac{dS_3}{dt}(t) = -\lambda_3(t) \quad (23)$$

$$\frac{dE_{3,1}}{dt}(t) = \lambda_3(t) - E_{3,1}(t) \quad (24)$$

$$\frac{dE_{3,2}}{dt}(t) = E_{3,1}(t) - E_{3,2}(t) \quad (25)$$

$$\frac{dE_{3,3}}{dt}(t) = E_{3,2}(t) - E_{3,3}(t) \quad (26)$$

$$\frac{dI_3}{dt}(t) = E_{3,3}(t-1) - \sigma_3 = I_3(t) - \sigma_3 \quad (27)$$

$$\frac{dR_3}{dt}(t) = \sigma_3(t) \quad (28)$$

※ supplementation

$$\lambda_3^g = S_3^g(t)\frac{T_{3,1}}{N_3^g}\alpha_1\omega\left(T_{1,1}E_1(t) + T_{2,1}E_2(t) + T_{3,1}E_3(t) + T_{4,1}E_4(t)\right)$$
$$+S_3^g(t)\frac{T_{3,2}}{N_3^g}\alpha_2\omega\left(T_{1,2}E_1(t) + T_{2,2}E_2(t) + T_{3,2}E_3(t) + T_{4,2}E_4(t)\right)$$
$$+S_3^g(t)\frac{T_{3,3}}{N_3^g}\alpha_3\omega\left(T_{1,3}E_1(t) + T_{2,3}E_2(t) + T_{3,3}E_3(t) + T_{4,3}E_4(t)\right)$$
$$+S_3^g(t)\frac{T_{3,4}}{N_3^g}\alpha_4\omega\left(T_{1,4}E_1(t) + T_{2,4}E_2(t) + T_{3,4}E_3(t) + T_{4,4}E_4(t)\right) \quad (29)$$

$$\lambda_3^n = \alpha_3 h\omega\frac{S_3^n(t)}{N_3^n}E_3(t) \quad (30)$$

$$\lambda_3(t) = \frac{1}{2}(\lambda_3^g + \lambda_3^n) \quad (31)$$

$$E_3(t) = E_{3,1}(t) + E_{3,2}(t) + E_{3,3}(t) \quad (32)$$

$$\sigma_3(t) = \beta I_3(t) \quad (33)$$

Figure 4: SEIR model for Group 3

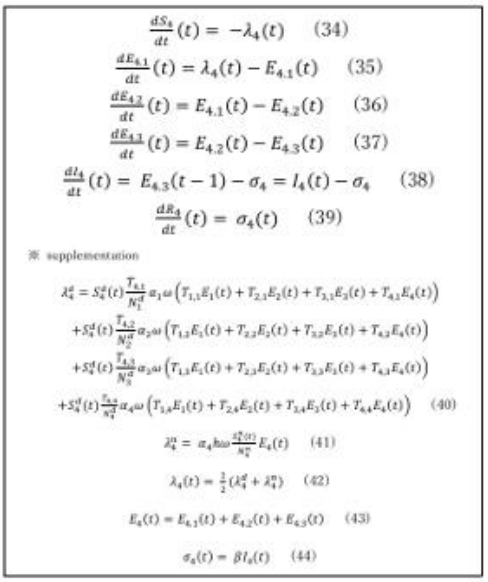

$$\frac{dS_4}{dt}(t) = -\lambda_4(t) \quad (34)$$

$$\frac{dE_{4,1}}{dt}(t) = \lambda_4(t) - E_{4,1}(t) \quad (35)$$

$$\frac{dE_{4,2}}{dt}(t) = E_{4,1}(t) - E_{4,2}(t) \quad (36)$$

$$\frac{dE_{4,3}}{dt}(t) = E_{4,2}(t) - E_{4,3}(t) \quad (37)$$

$$\frac{dI_4}{dt}(t) = E_{4,3}(t-1) - \sigma_4 = I_4(t) - \sigma_4 \quad (38)$$

$$\frac{dR_4}{dt}(t) = \sigma_4(t) \quad (39)$$

※ supplementation

$$\lambda_4^g = S_4^g(t)\frac{T_{4,1}}{N_4^g}\alpha_1\omega\left(T_{1,1}E_1(t) + T_{2,1}E_2(t) + T_{3,1}E_3(t) + T_{4,1}E_4(t)\right)$$
$$+S_4^g(t)\frac{T_{4,2}}{N_4^g}\alpha_2\omega\left(T_{1,2}E_1(t) + T_{2,2}E_2(t) + T_{3,2}E_3(t) + T_{4,2}E_4(t)\right)$$
$$+S_4^g(t)\frac{T_{4,3}}{N_4^g}\alpha_3\omega\left(T_{1,3}E_1(t) + T_{2,3}E_2(t) + T_{3,3}E_3(t) + T_{4,3}E_4(t)\right)$$
$$+S_4^g(t)\frac{T_{4,4}}{N_4^g}\alpha_4\omega\left(T_{1,4}E_1(t) + T_{2,4}E_2(t) + T_{3,4}E_3(t) + T_{4,4}E_4(t)\right) \quad (40)$$

$$\lambda_4^n = \alpha_4 h\omega\frac{S_4^n(t)}{N_4^n}E_4(t) \quad (41)$$

$$\lambda_4(t) = \frac{1}{2}(\lambda_4^g + \lambda_4^n) \quad (42)$$

$$E_4(t) = E_{4,1}(t) + E_{4,2}(t) + E_{4,3}(t) \quad (43)$$

$$\sigma_4(t) = \beta I_4(t) \quad (44)$$

Figure 5: SEIR model for Group 4

3 Methods

This section provides a precise and detailed elucidation of the parameter estimation process employed in this study, including the sources of data, the methodology for deriving specific parameters, and the tools and techniques utilized for experimentation and numerical analysis.

In estimating parameters such as initial values, data from a variety of sources were utilized. These included datasets published by the National Institute of Infectious Diseases (4); demographic and daytime mobility data for Saitama, Tokyo, Kanagawa, and Chiba prefectures (5); newly confirmed case data from the same regions (6); and vaccine efficacy data released by the Ministry of Health, Labour and Welfare (7). These data were employed to determine coefficients such as vaccine efficacy, infection rate, recovery rate, and mobility rate.

For numerical analysis, this study used nationwide infection data spanning from January 3, 2022, to April 10, 2022. This period was selected because the surge in COVID-19 cases during this time was attributed to the BA.1 lineage of the Omicron variant, while the emergence of the BA.2 lineage—with distinct epidemiological characteristics—was anticipated to occur subsequently. Although these variants are collectively referred to as COVID-19, differences in lineage may result in significant variations in infection rates, recovery durations, and latent periods. Accordingly, the present study focuses on the BA.1 lineage of the Omicron variant, which experienced a marked increase in transmission from the first through the fourteenth week of 2022.

Table 1: Parameters such as infection rates

character	meaning	numerical value
α1	Group 1 infection rate	0.213

α2	Group 2 infection rate	0.149
α3	Group 3 infection rate	0.168
α4	Group 4 infection rate	0.145
$T_{1.1}$	of those who stay in group 1	0.967
$T_{1.2}$	Movement rate from Group 1 to Group 2	0.01
$T_{1.3}$	Movement rate from Group 1 to Group 3	0.006
$T_{1.4}$	Movement rate from Group 1 to Group 4	0.017
$T_{2.1}$	Movement rate from Group 2 to Group 1	0.148
$T_{2.2}$	of those who stay in group 2	0.842
$T_{2.3}$	Movement rate from Group 2 to Group 3	0.004
$T_{2.4}$	Movement rate from Group 2 to Group 4	0.006
$T_{3.1}$	Movement rate from Group 3 to Group 1	0.118
$T_{3.2}$	Movement rate from Group 3 to Group 2	0.001
$T_{3.3}$	of those who stay in group 3	0.879
$T_{3.4}$	Movement rate from Group 3 to Group 4	0.002
$T_{4.1}$	Movement rate from Group 4 to Group 1	0.143
$T_{4.2}$	Movement rate from Group 4 to Group 2	0.008
$T_{4.3}$	Movement rate from Group 4 to Group 3	0.004
$T_{4.4}$	of those who stay in group 4	0.845
h	Prevalence of secondary infections within cohabiting families	0.35
β	recovery rate	0.1
ω	Efficacy of the new corona vaccine	0.5

The aforementioned parameters were computed through the following procedure. First, the daily number of newly confirmed cases in Saitama, Tokyo, Kanagawa, and Chiba prefectures was compiled using Excel, and the average of these figures was calculated. Subsequently, the differential equations constituting the SEIR model were algebraically rearranged so that only the infection rate remained on the left-hand side. By substituting empirical data—assigning Tokyo to Group 1, Saitama to Group 2, Kanagawa to Group 3, and Chiba to Group 4—the infection rates α_1, α_2, α_3, and α_4 were determined.

The estimation of the mobility rate T was based on population and daytime mobility data for each of the aforementioned prefectures.

The secondary infection rate within households, denoted as h, was derived with reference to data released by the National Institute of Infectious Diseases.

The efficacy of the COVID-19 vaccine, represented as ω, was established with reference to the interim report of the case-control study on vaccine effectiveness (Fourth Report), which evaluated the efficacy during the epidemic phases of Omicron sublineages BA.1/BA.2 and BA.5 (7).

As for the recovery rate β, considering the Omicron variant prevalent around January, the recovery period was estimated to be 10 days. Assuming that symptoms reliably resolve 10 days after onset, the daily recovery rate was set at 0.1 (8).

Experiments were performed using Python. RK45 was used to solve the simultaneous differential equations.

4 Results

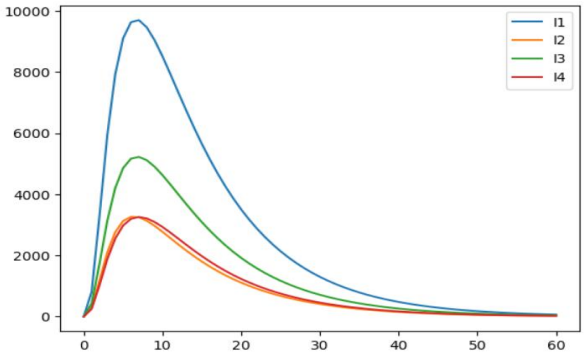

Figure 6: Simulation Results

This section concisely and lucidly presents the principal findings of the simulation, drawing comparisons with empirical data and underscoring the influence of inter-group mobility disparities on the peak number of new infections.

The simulation results are illustrated in Figure 7 above. In Group 1, the number of new infections reached its peak at 9,698 individuals on the 8th day from the onset of the simulation. In Group 2, the peak occurred on the 7th day, with 3,265 individuals newly infected. For Group 3, the apex was observed on the 8th day, amounting to 5,224 new cases. Similarly, Group 4 experienced its peak on the 8th day, with 3,258 newly infected individuals.

From January 5th to March 5th, the highest number of new infections occurred on the 32nd day in Tokyo, with 21,110 individuals affected, followed by Saitama Prefecture with 7,353 individuals on the same day, Chiba Prefecture with 6,599 individuals on the 37th day, and Kanagawa Prefecture with 9,096 individuals on the 32nd day.

Table 2: Simulation results with varying mobility rates

character	numerical	value		
$T_{1.4}$	1	0.25	0.7	0.1
$T_{1.2\sim4}$	0	0.25	0.1	0.3
$T_{2.1,3,4}$	0	0.25	0.1	0.3
$T_{2.2}$	1	0.25	0.7	0.1
$T_{3.1,2,4}$	0	0.25	0.1	0.3
$T_{3.3}$	1	0.25	0.7	0.1
$T_{4.1\sim3}$	0	0.25	0.1	0.3
$T_{4.4}$	1	0.25	0.7	0.1

Highest number of new infections				
Group1	15104.63	18458.88	16410.08	20061.35
Group2	4246.433	8576.16	6828.08	8776.14
Group3	8714.05	9963.21	10873.76	9612.22
Group4	6526.41	7985.38	8581.73	7488.35
Total Peak Number of New Infections from Group 1 to Group 4				
	34591.52	44945.8	42553.56	45925.33

Table 2 presents simulation results with variations in mobility across four patterns. When inter-group movement is the most frequent, the total peak number of new infections between each group is highest, whereas scenarios with no movement exhibited the lowest total peak number of new infections between groups.

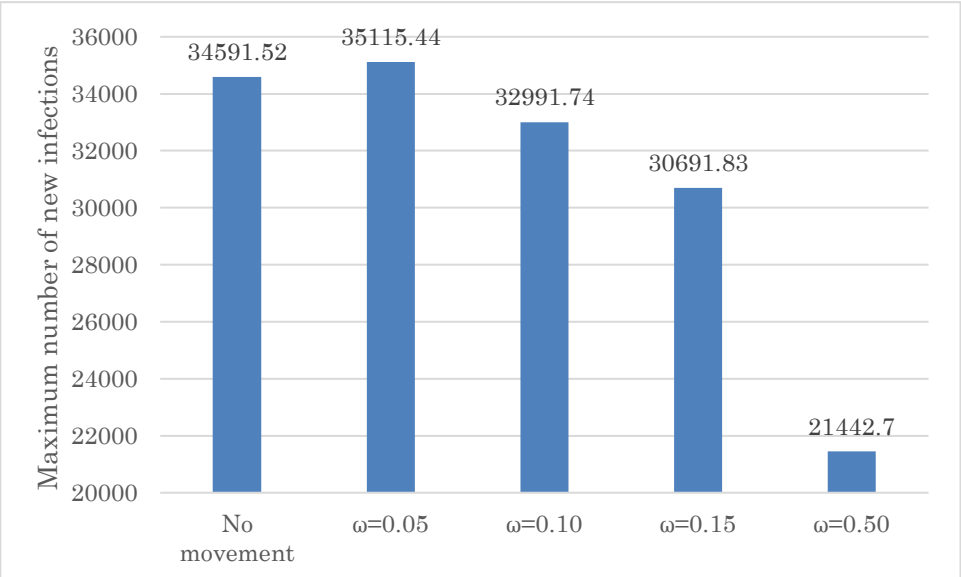

Figure 7: Comparison of the usefulness of migration control and vaccines

Finally, a comparative analysis was conducted to evaluate the infection-suppressing effects of human mobility restrictions versus the immunological benefits conferred by vaccination. As indicated in Table 2, an increase in human mobility generally correlates with a rise in the number of infections. Accordingly, based on empirical data from the four prefectures referenced in this study, we examined the extent to which the effectiveness of vaccination could justify accepting the risks associated with increased movement, thereby still contributing to the containment of the outbreak. The findings revealed that a vaccine efficacy of approximately 10% is sufficient to significantly mitigate the spread of infection, even when some degree of population movement is present.

5 Discussion

The simulation results deviated from the trends observed in actual data. In all scenarios, the peak of new infections occurred earlier, and the subsequent decline in cases transpired more rapidly than in the empirical data.

One possible explanation for the earlier emergence of peaks in both new infections and recoveries within the simulation results is the model's omission of critical real-world factors, such as immunity acquisition following recovery and the collapse of the healthcare system due to an overwhelming surge in cases. These omissions may have led to an accelerated progression and resolution of the outbreak within the simulations. Additionally, the discrepancies in the peak number of new infections are likely attributable to the model's exclusive focus on movement among the four predefined groups and its overly rigid separation of daytime activity and nighttime residence. In reality, individuals commute to Tokyo from prefectures beyond Saitama, Kanagawa, and Chiba, and international movement also plays a role. Moreover, infection rates can vary significantly depending on location. For instance, it is unreasonable to assume identical transmission probabilities in outdoor walkways, office environments, restaurants, and nightlife venues. The exclusion of these elements from the model likely contributed to the divergence between the simulation outcomes and real-world data.

Furthermore, an analysis of scenarios with varying mobility rates, as shown in Table 2, revealed that movement into high-infection-rate groups resulted in approximately a 1.3-fold increase in the number of new infections compared to scenarios with no intergroup movement. During the COVID-19 pandemic, refraining from non-essential outings significantly contributed to infection prevention.

Lastly, a comparative evaluation of the infection-suppressing effects of mobility restrictions versus immunity acquisition through vaccination indicated that the latter yields a more substantial reduction in infection spread. This finding suggests that enhancing individual immunity through vaccination may be more effective in mitigating the spread of infection than implementing mobility restrictions.

6 Conclusion

In order to address three pivotal questions—namely, the extent to which human mobility contributes to the spread of infection, the efficacy of vaccination, and whether mobility restriction or vaccine administration is more effective in curbing transmission—this study conducted simulations based on an SEIR model that incorporates variations in contact rates due to daytime and nighttime mobility, as well as the protective effects of vaccination. To enhance the realism of the simulation settings, data from the National Institute of Infectious Diseases (4), daytime mobility data for residents of Saitama, Tokyo, Kanagawa, and Chiba prefectures (5), publicly available data on new infections in these four regions (6), and statistics provided by the Ministry of Health, Labour and Welfare (7) were utilized. These data were employed to establish initial intergroup values and to calculate the model parameters by substituting them into the SEIR model’s differential equations.

The simulation outcomes displayed a degree of divergence from empirical data. Moreover, subsequent simulations that varied intergroup mobility rates revealed that when individuals from low-infection-rate groups refrained from moving to high-infection-rate groups, the peak number of new infections was approximately 1.3 times lower than in the scenario involving such movement. This finding suggests that human mobility can significantly influence the dynamics of infectious disease spread. Hence, it may be posited that policy measures aimed at reducing mobility could play a substantial role in mitigating outbreaks.

Additionally, a comparative analysis was conducted to evaluate the infection-suppressing effects of mobility restriction versus those of immunity acquisition through vaccination. The results indicated that vaccination conferred a more pronounced effect in curbing the spread

of infection. Therefore, even when considering the risks associated with movement, the act of administering vaccines appears to offer greater benefits in preventing large-scale transmission.

It should be noted, however, that this study does not take into account factors such as the mobility of individuals beyond the four predefined groups, the possibility of reinfection following natural immunity, demographic changes due to births and deaths, or healthcare system collapse resulting from overwhelming infection rates. Constructing an enhanced model that integrates these additional variables and conducting simulations that more closely reflect real-world conditions remain important directions for future research.

Acknowledgement

This research was partially supported by Grants-in-Aid for Scientific Research (C) 22K02147 and (B) 23K21016.

References

[1] W. O. Kermack and A. G. McKendrick, Contributions to the mathematical theory of epidemics-I, Proceedings of the Royal Society, 1927, 115A: 700-721

[2] H. Inaba, Mathematical Models of Infectious Diseases, bafukan,2022

[3] R. Sakamaki, S. Fujita, SIR Model with the Person Trip to Analyze the Epidemic of Influenza, Proceedings of the 7th IIAE International Conference on Intelligent Systems and Image Processing, 2019

[4] National Institute of Infectious Diseases, "Transition of Secondary Infection Rate by Period of Variant Strain Epidemic in COVID-19", https://www.niid.go.jp/niid/ja/2019-ncov/2502-idsc/iasr-in/11636-513c03.html, Accessed 1/10/2024.

[5] e-stat, Japan in Statistics, https://www.e-stat.go.jp/stat-search/files?page=1&layout=datalist&toukei=00200521&tstat=000001136464&cycle=0&tclass1=000001136469&result_page=1&tclass2val=0, 4/10/2024.

[6] Ministry of Health, Labour and Welfare, Open Data, https://www.mhlw.go.jp/stf/covid-19/open-data.html, 4/6/2025.

[7] Ministry of Health, Labour and Welfare, Tentative report of a case-control study of the efficacy of a novel corona vaccine (Report 4): Omicron strain (BA.1/BA.2 and BA.5) during an outbreak(BA.1/BA.2 and BA.5) during the epidemic period, https://www.mhlw.go.jp/content/10900000/000977543.pdf, 3/28/2025.

[8] Ministry of Health, Labour and Welfare, Revision of Discharge Criteria and Removal Criteria, https://www.mhlw.go.jp/content/000639696.pdf, 12/28/2024.